Chapter 3

Synthesis of Nanomaterials for Immunosensor Platforms

3.1 Introduction

The use of metallic nanomaterials such as gold, platinum, and silver had greatly influenced the performance of biosensors [96]. The focus of research in using metallic nanomaterials for biosensors has been on achieving highly controllable size and thus modulating conductivity, shape, and physicochemical characteristics of these. Several studies had described the conjugation of metallic nanomaterials with polymers and bioactive molecules (e.g., monoclonal antibodies) to enhance biocompatibility. Due to their unique properties, these bio-sensing platforms were utilized in the development of electrochemical biosensors. The research attention to metal nanoparticles has also been raised due to their easy synthesis, characterization, and surface functionalization, which are critical in biomedical applications. The surface functionalization of metal nanoparticles has considerable potential for their realization in use for clinical applications [97].

In recent years, bimetallic nanoparticles have owned dual characteristics relative to parental metals. Since these properties strongly depend on the shape, size, and nanoparticle's composition ratio. Extensive scientific studies have been carried out on bimetallic core-shell and alloy nanoparticles' composition, formation, and size-controlled synthesis. Many methods have been used to synthesize bimetallic nanoparticles: alcohol, citrate reduction [98], alcohol reduction [99], solvent extraction reduction [100], sonochemical method [101], electrolysis of a bulk metal [102], laser ablation [103] and chitosan initiated in-situ reduction approach [104]. Among all these, chitosan initiated in-situ reduction approach is a typical

technique to prepare bimetallic metallic nanoparticles in solution by reducing their ionic salts. Chitosan is a naturally occurring polysaccharide with excellent biodegradable and biocompatible characteristics. Using chitosan as a reducer and stabilizer will not introduce any toxicity or biological hazards because it is environmentally friendly [105]-[106]. This synthesis process is known in 12 fundamental principles of green chemistry that have been used in the synthesis and growth of biological and biomimetic materials with desirable properties [107].

In-situ reduced nanoparticles impregnated in the chitosan network improve charge transmission, enable more precise functionalization, and improve biocompatibility. The in-situ reduced nanoparticles could have a more uniform distribution and improved chemical coordination inside the chitosan network. Therefore, this reduction technique has an advantage over those that use a physical mixing of polymeric materials and nanoparticles. Thus, the synthesis of composites of polymer and metal was done by in-situ reduction of gold chloride in the presence of chitosan, and their coating on a working electrode was achieved for developing platforms to use in an electrochemical immunosensor. It is hypothesized that the composite material prepared through in-situ reduction of gold chloride has better chemical coordination and homogeneous distribution in the chitosan network, which has advantages over the methods that adopt the physical mixing of nanoparticles with polymeric materials [93]. The formulation also has the advantage of achieving stable and adhesive coatings on working electrodes to develop platforms for monoclonal anti-glutamate antibody immobilization. The availability of GNP in composite material used for coating on working electrodes has enhanced functionalization capability and improved charge transportation towards developing a high-sensitivity biosensor [108].

3.2 Synthesis of Gold-Chitosan Nanocomposites (CS-GNP)

3.2.1 Preparation of Gold Nanoparticles Through Chitosan Reduction

Chitosan, having randomly distributed β-linked D-glucosamine and N-acetyl-D-glucosamine, was obtained from Sisco Research Laboratories (SRL) with a degree of deacetylation of 90%, and it was dissolved in deionized (DI) water from a Millipore system (18.2 MΩ) at various w/v ratio with acetic acid. The mixtures were stirred and heated to 55-60°C until a clear solution was obtained. A freshly prepared gold chloride ($AuCl_3$) solution was added to the chitosan solution, and the reaction was monitored in a time-dependent manner by obtaining UV-visible spectra with the use of a Shimadzu UV-visible spectrophotometer (Tokyo, Japan). Four different concentrations of chitosan (3g w/v, 2 g w/v, 1g w/v and 0.5g w/v with acetic acid by also varying its proportion in the same ratio as 3 %, 2 %, 1 %, and 0.5 %) were used. A fixed amount of 0.4 mM of $AuCl_3$ was added to these different chitosan solutions. Then the mixture was kept at 60°C under magnetic stirring for the in-situ formation of gold nanoparticles within the chitosan network. The reaction was monitored by measuring the surface plasmon resonance (SPR) peak of GNP in the solution at various time points from 0 h to 7 h [108].

Figure 3.1 shows the time-dependent UV-visible spectra of a colloidal suspension of CS-GNP from the start of the reaction at 2 h, 4 h, 5 h, 6 h, and 7 h demonstrating the in-situ reduction of 0.4 mM of gold chloride through chitosan at four different concentrations. For the first 2 h of the reaction, there was no evidence for the formation of GNP through spectroscopic signature associated; however, further progression of the reaction at 4 h showed a significant appearance of SPR peak at 525 nm at the use of 2.0, 1.0, and 0.5% w/v of chitosan. The SPR peak intensity gradually increased with the progression of reaction time

and stabilized after 7 h of reaction time for all the conditions used in the experiment. The higher chitosan concentration (3% w/v) did not show the appearance of GNP SPR peak even for a reaction progression time of 7 h.

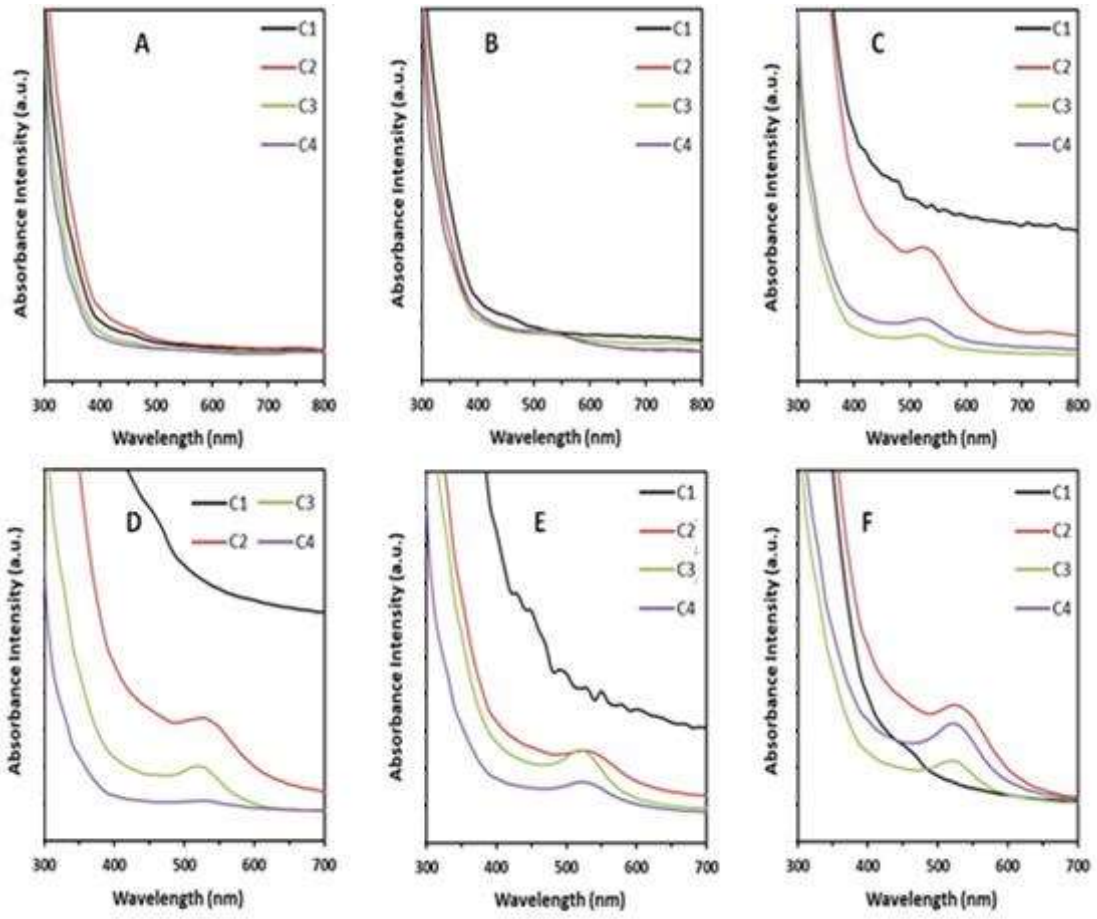

Figure 3.1: *UV-vis spectra of CS-GNP colloidal suspension at various time (T) points (A) start of the reduction T = 0 h, (B) T = 2 h, (C) T = 4 h, (D) T = 5 h, (E) T = 6 h and (F) T = 7 h during in-situ reduction of 0.4 mM gold chloride at various concentration (C1 = 3g w/v, C2 = 2g w/v, C3 = 1g w/v and C4 = 0.5g w/v) of chitosan.*

The relative proportion of GNP in the colloidal suspension was estimated by taking the difference in absorbance intensities at λ_{SPR} and λ_{450} in UV-vis spectra of chitosan-GNP [109]. The use of 1% w/v of chitosan in 0.4 mM of gold chloride showed a GNP surface plasmon

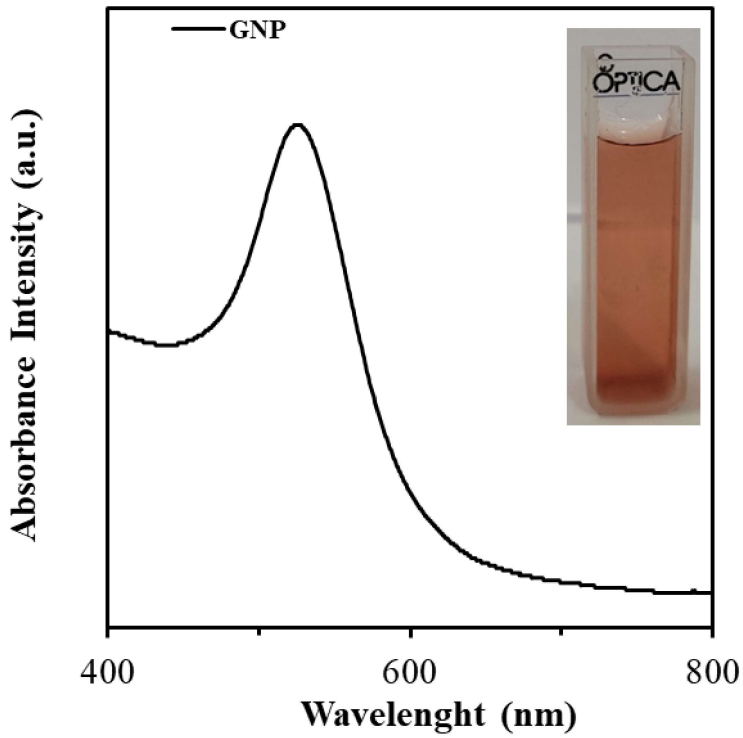

Figure 3.2: *UV-vis spectrum of CS-GNP gel solution.*

resonance peak (λ_{SPR}) at 526 nm after 4 h of the reduction reaction. Further, an increase in the peak intensity was observed with the progression of reaction time and reached saturation after 24 h. This optimized condition of 0.4 mM of gold chloride with 1 % w/v of chitosan and 24 h of reaction time further investigated physicochemical properties and coating on working electrodes for developing electrochemical biosensors. **Figure 3.2** shows GNP λ_{SPR} at 526 nm in the UV-vis spectrum of a colloidal suspension of CS-GNP with a homogeneous appearance of red color without any sedimentation or agglomeration for the optimized conditions used for further studies.

FTIR spectra of chitosan and chitosan-reduced gold nanoparticles were recorded on the KBr matrix with Thermo Scientific Nicolet iS5 system from 400 to 4000 cm^{-1} with a scan rate of 64 and 4 resolution steps. FTIR spectra of chitosan and CS-GNP had shown the presence of

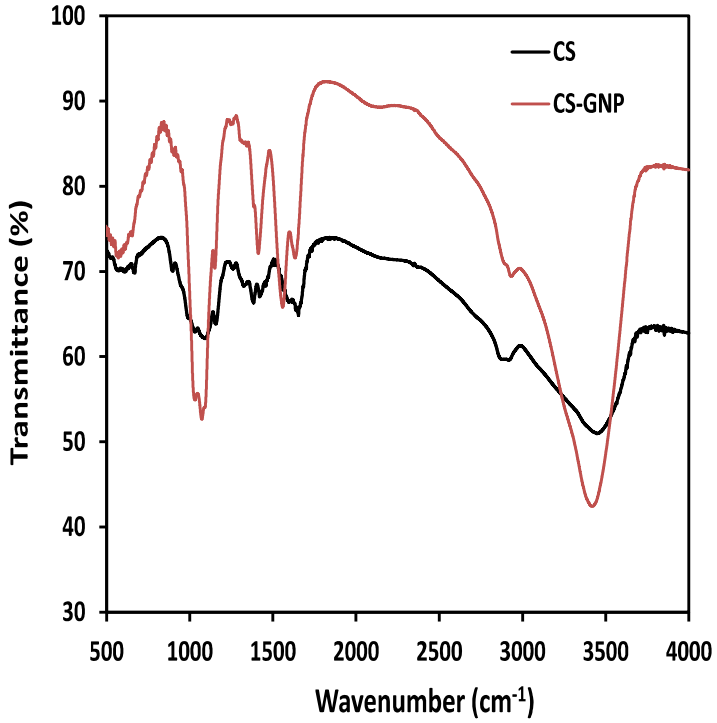

Figure 3.3: *FTIR spectra of CS and CS-GNP gel solution.*

functional moieties of chitosan and corresponding changes due to the reduction of gold chloride during the formation of GNP. The blue shift of the peak for the amino group N-H bending at 1579 cm^{-1}, C-N stretching at 1318 cm^{-1}, and N–H rocking vibration at 895 cm^{-1} in the FTIR spectrum of CS-GNP was observed. This shift indicates the coordination of GNP within the chitosan network, possibly due to the electrostatic interaction between chitosan moieties and surface charge on gold nanoparticles [88,89].

3.2.2 Structural Properties of CS-GNP Composites

XRD patterns of chitosan and CS-GNP film surfaces were obtained by recording X-ray diffraction patterns with the use of a Rigaku mini Flex-600 X-ray diffractometer with Cu Kα radiation (λ=1.5418 Å). The scan was carried out at a speed of 2°/min and 2θ range from 0 to 80°. **Figure 3.4 A** shows the XRD pattern of GNP and CS-GNP. Two distinct characteristic

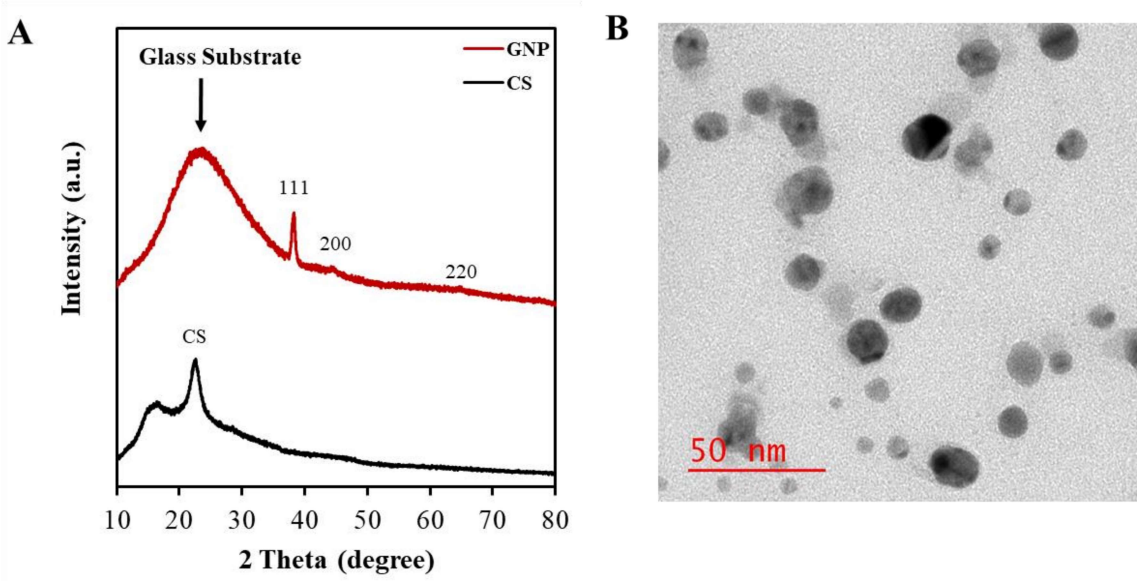

Figure 3.4: *(A) XRD patterns of CS and CS-GNP film, and (B) TEM image of CS-GNP.*

peaks at the 2θ value of 16.9° and 22.7° in XRD spectra of chitosan were obtained, and these correspond to (002) and (101) crystallographic planes of chitosan molecules respectively. The CS-GNP XRD pattern showed very low-intensity GNP peaks at 2θ values of 38.4° (111) and 44.8° (200). The position of the GNP peak in XRD spectra is attributed to the face-centered cubic structure of GNP. XRD of GNP alone was not obtained due to their colloidal suspension nature, and the peak corresponding to gold in CS-GNP was identified, which coincides with the previous literature [112]. Additionally, the 2θ peak in CS-GNP XRD

spectra corresponding to chitosan had shifted towards a higher 2θ value. The shift and increase in broadening of the XRD peak of the CS-GNP composite could be associated with a decrease in crystallinity in crystallographic planes of chitosan [108]. An average diameter of ~15 nm with the spherical-shaped GNP within the chitosan was observed in the TEM image (**Figure 3.4 B**). The TEM image confirmed the presence of a uniform distribution of GNP within the chitosan network.

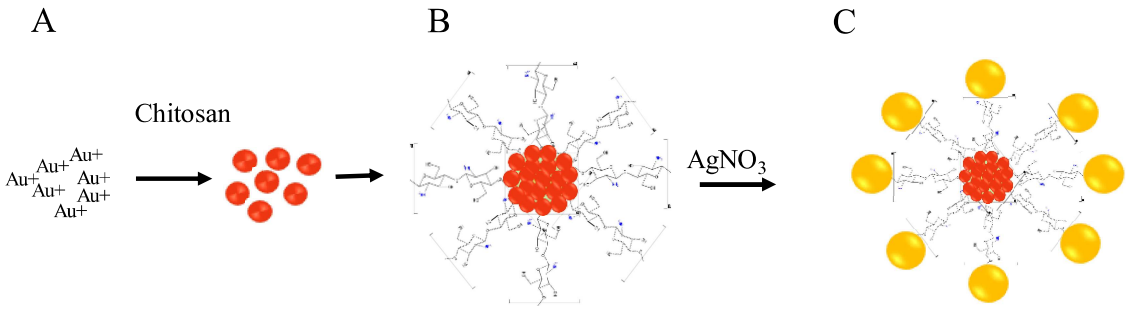

Figure 3.5: ***(A)*** *Schematic representation of GNPs synthesized from $AuCl_3$/CS,* ***(B)*** *Schematic representation of GNP,* ***(C)*** *Schematic representation of DMC nanoparticles,*

3.3 In-situ Reduction Dual-metallic Conjugate Through Polymer Linkage

A green synthesis method is used for preparing gold nanoparticles, silver nanoparticles, and duel metal conjugate of CS-GNP-AgNP (D2) and CS-AgNP-GNP (D3) by a two-step process. Here, chitosan acts as a reducing agent and reduces $AuCl_3$ and $AgNO_3$ salts to zerovalent GNP and AgNP nanoparticles without any additional stabilizer [113]. Chitosan is a naturally occurring polysaccharide with excellent biodegradable and biocompatible characteristics. Using chitosan as a reducer and stabilizer will not introduce any toxicity or biological hazards [114]. The optical properties, structures, and morphologies of gold nanoparticles, silver nanoparticles, CS-GNP-AgNP (D2), and CS-AgNP-GNP (D3)

nanoparticles were characterized by UV-vis spectroscopy, FTIR, XRD, and TEM. The electrochemical behavior of NPs and DMC was investigated using cyclic voltammetry.

3.3.1 Synthesis of AgNP

All glassware used was cleaned in a batch of freshly prepared Aqua Regia solution (HCl: HNO_3 3:1) and then rinsed thoroughly with DI, followed by 70% ethanol. Before preparing silver nanoparticles, the stock solutions of chitosan with medium molecular weight were prepared by dissolving one gram of chitosan in 100 ml DI water with 1% acetic acid solution.

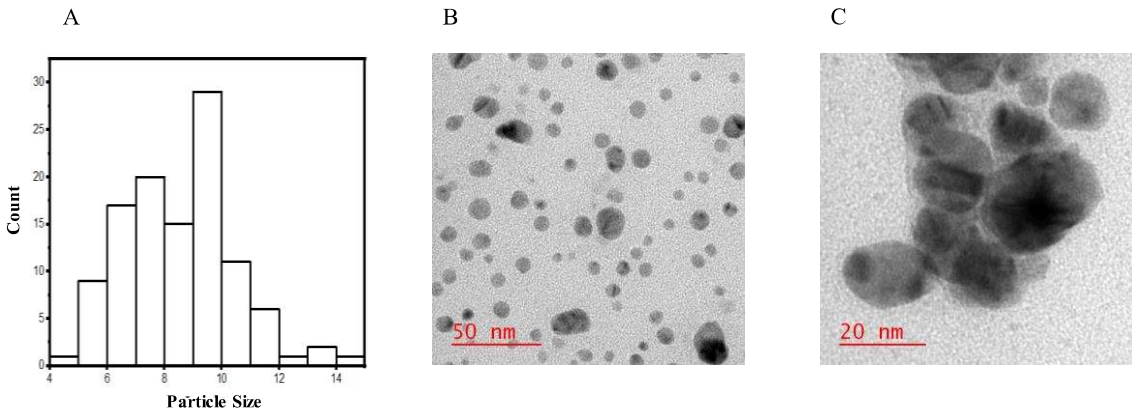

Figure 3.6: ***(A)*** *Particle size distribution bar graph for GNP,* ***(B)*** *Transmission electron microscopy image of GNP,* ***(C)*** *Transmission electron microscopy image of DMC nanoparticles.*

Due to the poor solubility of chitosan, the mixture was vortexed and heated to 50°C under magnetic stirring for about 1 hour until a clear solution was obtained. When used in the experiments, the stock solution was diluted to the needed concentration. In a dark room, a white color powder of $AgNO_3$ (0.2 mM) was mixed with the chitosan solution, and then the mixture was heated to 60°C under magnetic stirring until a dark brown colloidal suspension

was obtained. The chitosan concentration adjusts the reaction time, although a 10 to 15 h reaction time is enough.

3.3.2 CS-GNP-AgNP Dual Metal Conjugation Through Polymer Linkage

Two milliliters of gold nanoparticles are diluted with 8 ml DI water in a 30 ml cell culture tube and heated to 60°C under magnetic stirring for about 1 hour until a continuous solution is obtained. Then add 0.2 mM of $AgNO_3$ followed by 8 ml of chitosan solution and continuously heat to 60°C under magnetic stirring overnight.

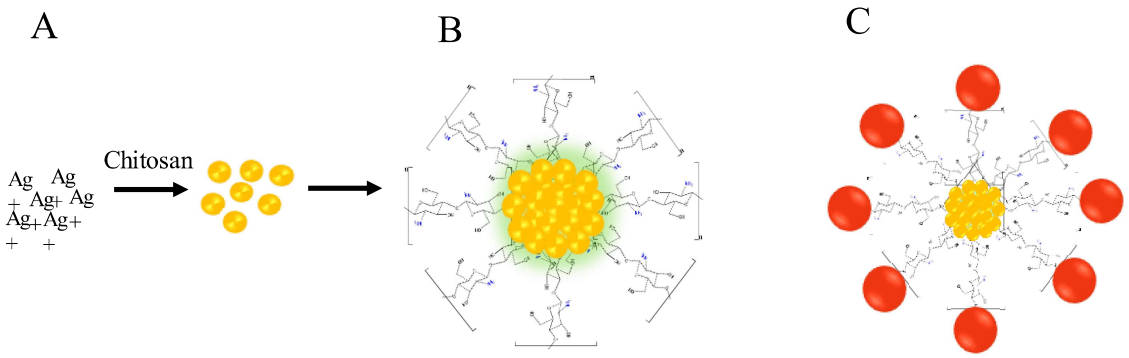

Figure 3.7: ***(A)*** *Schematic representation of AgNP's synthesized from $AgNO_3$/CS,* ***(B)*** *Schematic representation of AgNP,* ***(C)*** *Schematic representation of DMC nanoparticles.*

3.3.3 CS-AgNP -GNP Dual Metal Conjugation Through Polymer Linkage

Two milliliters of silver nanoparticles are diluted with 8 ml DI water in a 30 ml cell culture tube and heated to 60°C under magnetic stirring for about 1 hour until a continuous solution is obtained. Then add 0.2 mM of $AuCl_3$ followed by 8 ml of chitosan solution and continuously heat to 60°C under magnetic stirring overnight.

3.3.4 Physico-chemical Characteristics

To synthesize the GNP, the CS solution was first mixed with $AuCl_3$. CS reacted with the Au^+ ion to form metallopolymer $[Au/CS]^+$. This metallopolymer was stirred at a moderate temperature of 60°C according to varying stirring times to form Au/CS colloidal suspension. In this process, Au^+ was successfully reduced to Au^0 to form gold nanoparticles. Schematically represented in **Figures 3.5 A** and **B.** Surface Plasmon Resonance (SPR) in the UV–vis spectrum is observed at 526 nm **(Figure 3.9 (b))** indicating that the gold nanoparticle dispersion was synthesized successfully and effectively stabilized. The TEM analysis **(Figure 3.6 B)** revealed the presence of reasonably uniform spherical gold

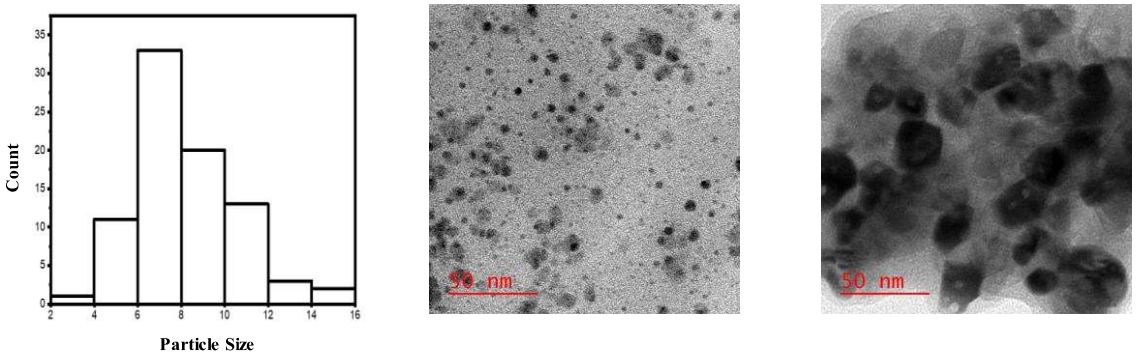

Figure 3.8: ***(A)*** *Particle size distribution bar graph for AgNP,* ***(B)*** *Transmission electron microscopy image of AgNP,* ***(C)*** *Transmission electron microscopy image of DMC nanoparticles.*

nanoparticles with an average particle diameter in a range from 8 nm to 10 nm as calculated by the ImageJ software **(Figure 3.6 A)**. The XRD pattern of GNP is shown in **(Figure 3.10 (b)),** which shows pecks at 2θ values of 38.4° (111), 44,8° (200), 65.4° (220), and 77.4° (311). These peck positions indicated the formation of GNP in a single phase and matched JCPDS file no 652870. The crystal structure was found to be simple cubic. To synthesize

the dual metal conjugate, $AgNO_3$ is added to the GNP solution; CS reacts with the Ag^+ ion to form a metallopolymer $[Ag/CS]^+$.

This metallopolymer was stirred at a temperature of 60°C according to varying stirring times to form CS-GNP-AgNP dual metal conjugate. In this process, Ag^+ was successfully reduced to Ag^0 to form an AgNP layer on the GNP and schematically represented in **Figures 3.5 C.** UV–vis plots in **Figure 3.9 C** show that a GNP SPR shifts from 526 nm to 471 nm After the AgNP layer is deposition. A broad peck was obtained ranging from 410 nm to 540 nm. This change illustrated the successful synthesis of CS-GNP-AgNP dual metal conjugate. The TEM analysis **(Figure 3.6 C)** revealed the presence of reasonably uniform spherical CS-GNP-AgNP dual metal conjugate of a particle diameter of 20 nm

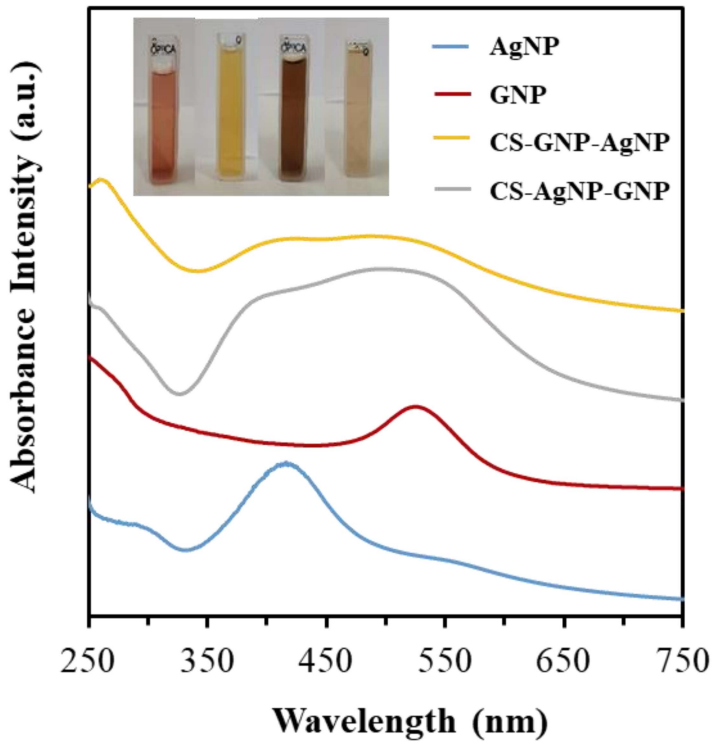

Figure 3.9: *UV-vis spectra of a) gold nanoparticles (GNP), b) silver nanoparticles (AgNP), c) CS-GNP-AgNP, and d) CS-AgNP-GNP.*

with a standard deviation of ±2 nm. The XRD pattern of CS-GNP-AgNP dual metal conjugate is shown in **(Figure 3.10).** Peaks were obtained at 2θ values of 9.4°, 27.2°, and 45.8°. For the synthesis of silver nanoparticles, $AgNO_3$ was added to the CS solution then it reacted with the Ag^+ ion to form a metallopolymer $[Ag/CS]^+$. This metallopolymer was stirred at a temperature of 60°C according to varying stirring times to form Ag/CS nanocomposites. In this process, Ag^+ was successfully reduced to Ag^0 to form AgNP. SPR at 416 nm in the UV–vis spectrum **(Figure 3.9)** was a clear indication that the dispersion was effectively stabilized. The TEM analysis **(Figure 3.8 B)** revealed the presence of reasonably uniform spherical AgNP of the average particle diameter of 8 nm with a standard deviation of ±2 nm. The XRD pattern of AgNP is shown in **Figure 3.10.**

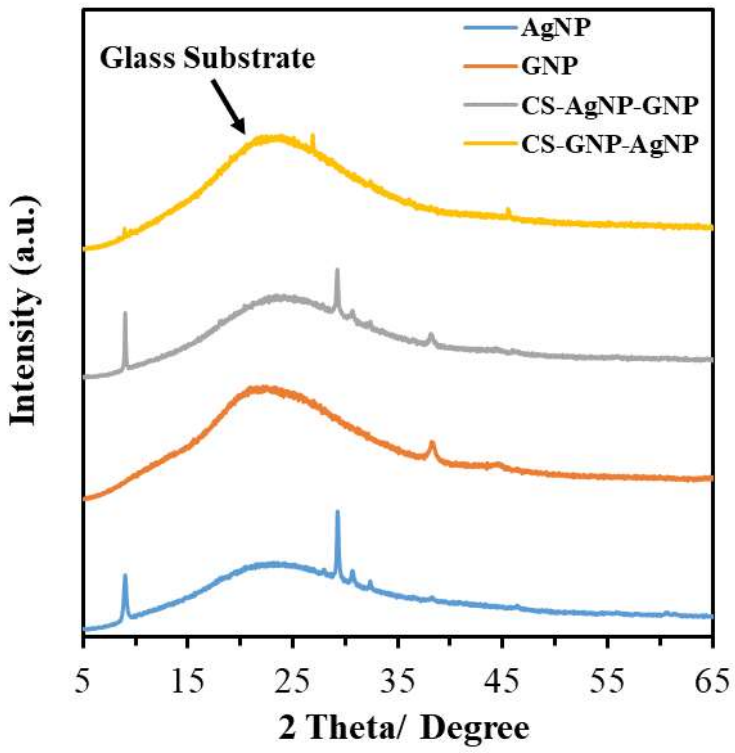

Figure 3.10: *XRD pattern of a) gold nanoparticles (GNP), b) silver nanoparticles (AgNP), c) CS-GNP-AgNP, and d) CS-AgNP-GNP.*

Major peaks were observed at 2θ values of 9°(CS), 28.12° (210), 29.4° (211), 30.6° (022), 32.4° (122), and 46.5° (123) and matched to JCPDS File No. 840713. The crystal structure was found to be simple cubic. When $AuCl_3$ was added to the AgNP solution then CS reacted with the Au^+ ion to form metallopolymer $[Au/CS]^+$. This metallopolymer was stirred to form a GNP layer onto the AgNP. Illustrated schematically in **Figures 3.7 A, B,** and **C**. In UV–vis spectra **(Figure 3.9),** the SPR of AgNP swifts from 416 nm to 498 nm as the GNP layer increases the overall size. A brode peck is obtained from 350 nm to 550 nm, which indicates the formation of CS-AgNP-GNP dual metal conjugate. The TEM analysis **(Figure 3.8 C)** revealed the presence of reasonably uniform spherical CS-AgNP-GNP dual metal conjugate with a particle diameter of 15-25 nm with a standard deviation of ±2 nm.

The XRD pattern of CS-AgNP-GNP dual metal conjugate is shown in **Figure 3.10,** and Peaks were obtained at 2θ values of 9°(CS), 29.4° (211), 30.6° (022), 32.4° (122) and 38.4° (111), 44.8° (200). And matched with JCPDS File No. 840713 and 652870).

3.3.5 Electrochemical Characteristics

For the electrochemical study, a glassy carbon electrode **(**GCE) was used as the working electrode platform. GCE was cleaned with 0.3 μm and 0.05 μm micropolish alumina (Buehler, USA), followed by a 30 min sonication in ethanol and water [115] to obtain a clean and impurity-free surface. After that, the GCE was dried at room temperature. 10 μL of chitosan, gold nanoparticles, silver nanoparticles, CS-GNP-AgNP, and CS-AgNP-GNP were drop-casted onto the clean surface of 3 mm GCE, respectively. Modified GCE were dried at room temperature for 12 h.

Cyclic voltammetry (CV) of GNP, AgNP, CS-AgNP-GNP, and CS-GNP-AgNP dual metal conjugate were carried out in 100 mM PBS solution having a pH value of 7.4, containing

five mM $K_4[Fe(CN)_6]$ and 0.1M KCL, Ag/AgCl as the reference electrode, and Pt wire as the counter electrode. Voltage is cycled between -0.3 to 0.9 V with a sweep rate of 30 mV s^{-1} with continuous purging of 99% pure nitrogen gas[116]. 10 µL of each nanoparticle were dropped and cast onto the clean surface of 3 mm GCE. Modified GCE is used as the working electrode, Ag/AgCl as the reference electrode, and Pt wire as the counter electrode. Voltage is cycled between -0.3 to 0.9 V with a sweep rate of 30 mV s^{-1} with continuous purging of 99% pure nitrogen gas. Anodic (I_{pa}) and cathodic (I_{pc}) peak currents of the GNP in cyclic voltammetry response showed a four-fold increase as compared to chitosan, respectively. I_{pa} and I_{pc} of CS-GNP-AgNP dual metal conjugate were again increased from ~ 20 µA to ~ 30 µA and ~ 17 µA to ~ 25 µA.

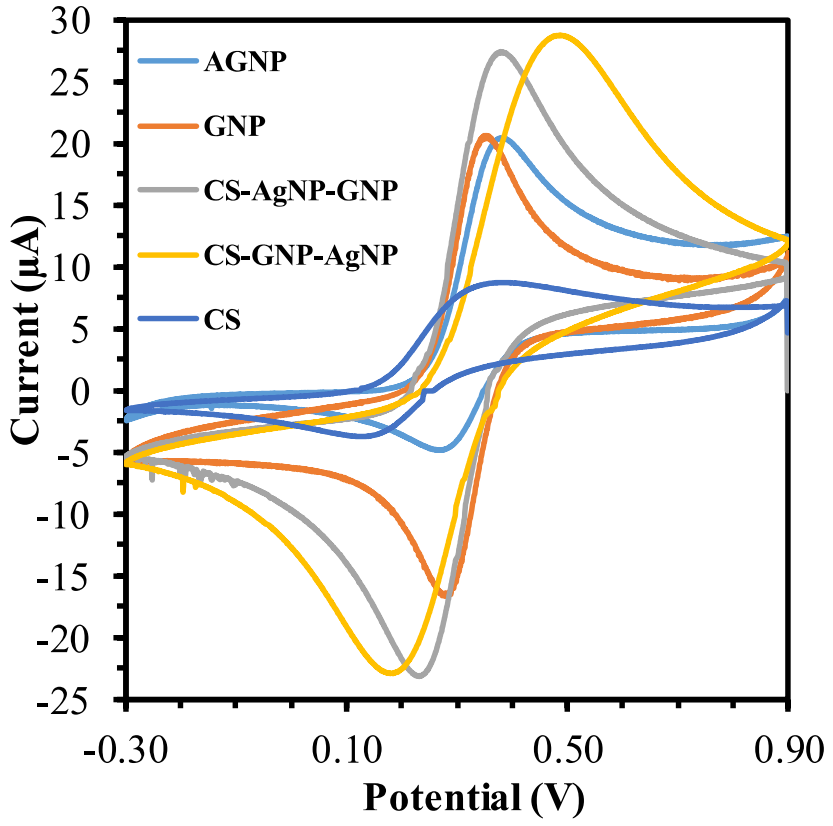

Figure 3.11: *Cyclic voltammogram of a) gold nanoparticles, b) silver nanoparticles, c) CS-GNP-AgNP, and d) CS-AgNP-GNP.*

The conductivity enhancement was seen due to conducting nature of silver, which may have helped in the fast electron transfer process between the electrolyte and the electrode, as shown in **Figure 3.11**. The electrochemical response of the AgNP shows a four-fold increase compared to chitosan in I_{pa}, while no change was observed in I_{pc}. In CS -AgNP-GNP dual metal conjugate, I_{pc}, and I_{pa} were increased from ~ 20 µA to ~ 28 µA and ~ 3 µA to ~ 23 µA. The conductivity enhancement was seen as an anodic current due to Gold's stable and conducting nature, which may have helped in the fast electron transfer process between the electrolyte and the electrode during the reduction reaction.

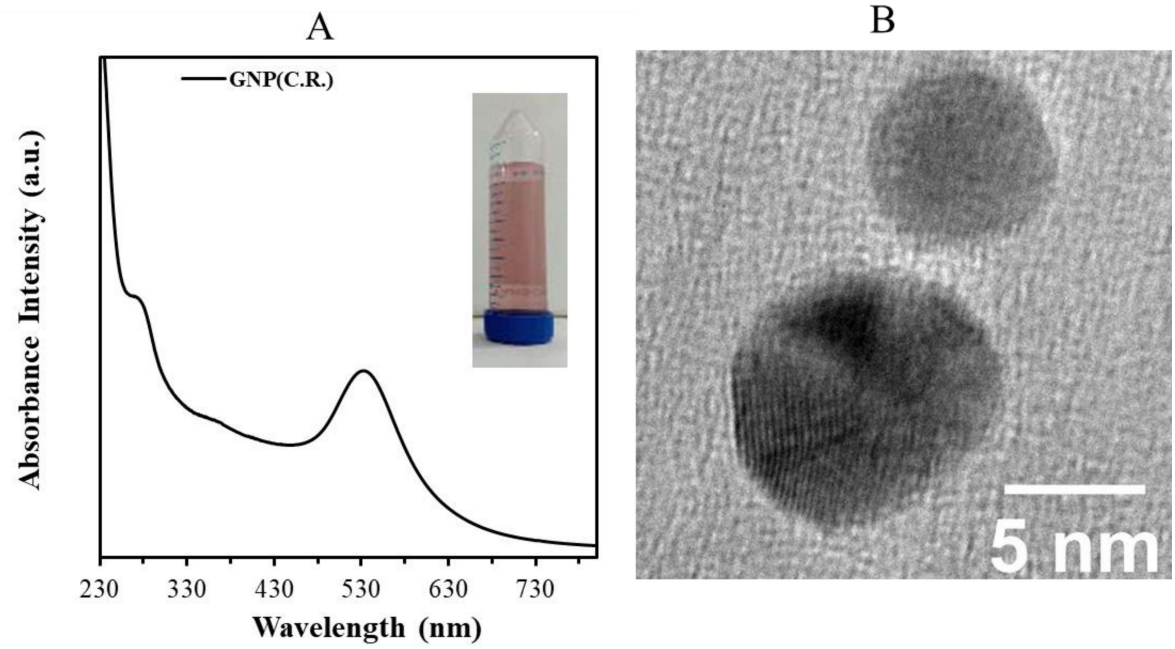

Figure 3.12: ***(A)*** *UV-vis spectrum GNP at 535 nm and optical image,* ***(B)*** *high-resolution TEM image of GNP.*

3.4 Synthesis of GNP Through Chemical Route

Gold chloride ($AuCl_3$) and lithium borohydride ($LiBH_4$) were purchased from Sigma-Aldrich. Deionized (DI) water from a Millipore system (~18.2MΩ cm) was used throughout the experiment. The preparation of gold nanoparticles, an aqueous solution of $AuCl_3$ (0.2 mM), and DI water was prepared, and then add 2 mM of Lithium Borohydride ($LiBh_4$) to the mixture at room temperature under magnetic stirring until a red solution was obtained [109]. The synthesized gold nanoparticles were prepared using $LiBH_4$ as a reducing agent without any stabilizers [50]. The GNP colloid disperses red color, which is confirmatory to its synthesis, and its UV-vis spectrum shows λ_{SPR} at 535 nm **Figure 3.12**.

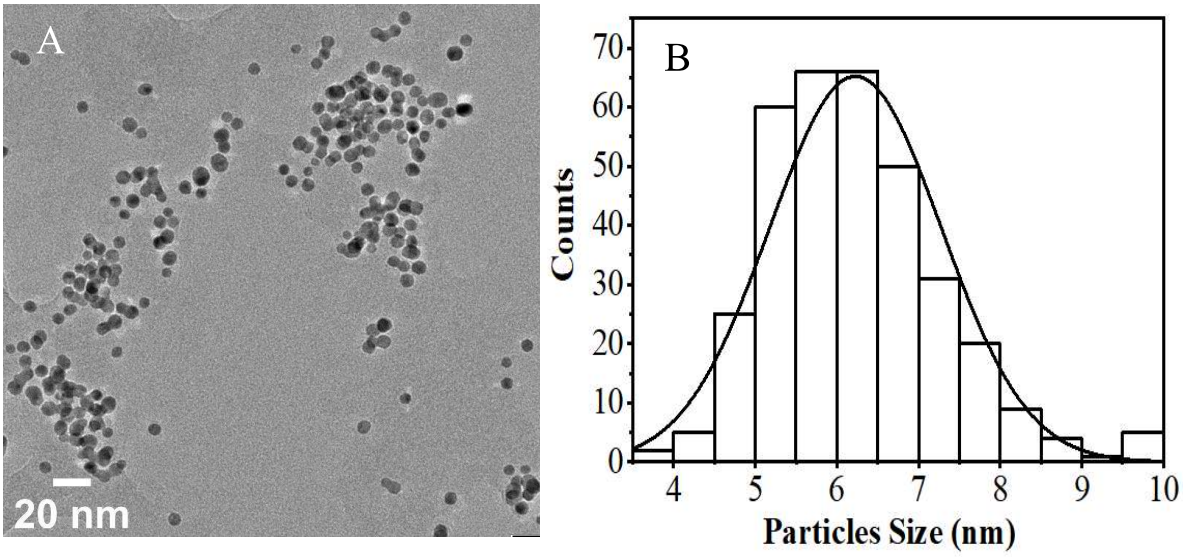

Figure 3.13: *(A) GNP colloid dispersion TEM image of GNP and (B) size distribution curve.*

The TEM image study of GNP in **Figure 3.13 A** indicates the uniform distribution of spherical gold particles. ImageJ software has been used to process the TEM image for measuring the size of the particles. **Figure 3.13 (B)** demonstrates an average diameter of ~

6 nm considering almost 150 Gold nanoparticles in a single image, as indicated in the size distribution curve of the ImageJ software. The curve has a gaussian-like distribution with a full-width half-maxima value of ~ 2.5 nm. **Figure 3.12 (B)** shows the high-resolution TEM image having interplanar spacing (d) ~ 0.24 nm for the (111) plane and ~ 0.20 nm for the (200) plane.

XRD analysis of GNP is shown in **Figure 3.14 (A)**. The XRD pattern showed the broad intensity of peaks due to the low concentration of GNPs in the film. The spectrum illustrates two distinct characteristic peaks at the 2θ value of 38.42° and 44.38°, which correspond to (111) and (200) crystallographic planes, respectively.

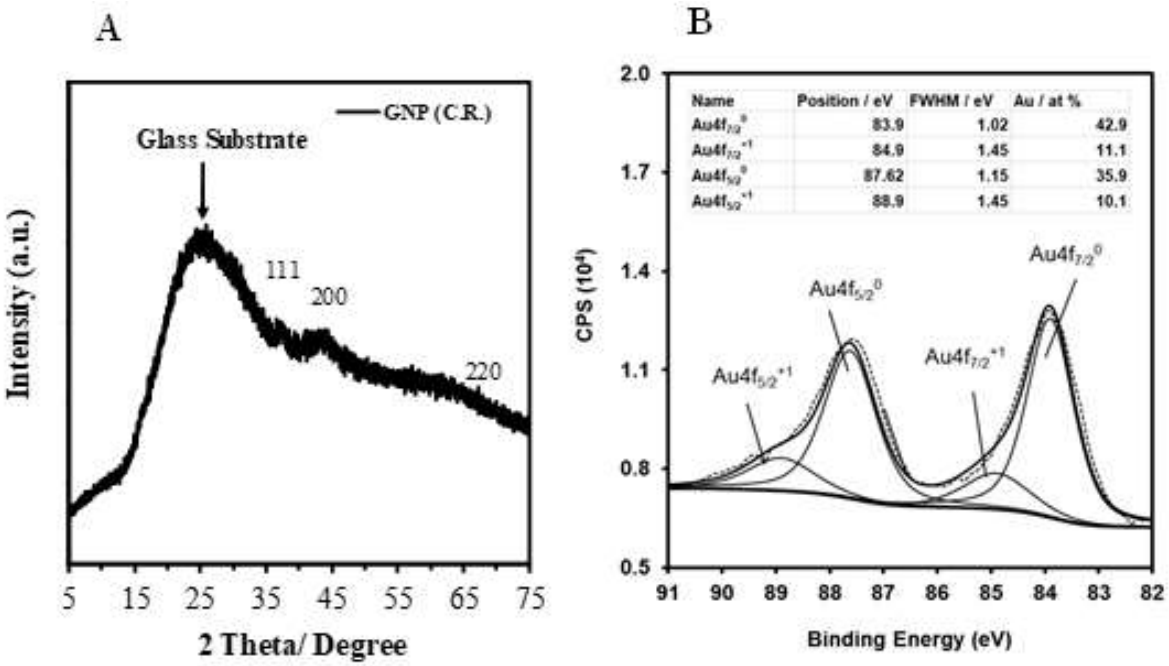

Figure 3.14: (A) *XRD patterns of GNP and* ***(B)*** *XPS Spectrum of GNP.*

The position of the GNP peak in the XRD spectrum is attributed to the face-centered cubic structure of GNP, which coincides with the previous literature (JCPDS 65-2870). The

analysis of XRD coincides with the outcomes of TEM. The thin film surface was identified using XPS analysis of GNP. The XPS elemental analysis of PANI-GNP shows 56.8%, 40.1%, 3.01 %, and 0.5% atomic % proportions of carbon, oxygen, nitrogen, and gold, respectively. The narrow scan X-ray photoelectron spectra of Au4 *f* in GNP are shown in **Figure 3.14 B.** The Au 4*f* spectrum in the GNP has peck at 83.9 and 87.62, which is matched with thiol monolayer-protected gold nanoparticles [110-112].